Science of the Total Environment 949 (2024) 175221

Contents lists available at ScienceDirect

Science of the Total Environment

journal homepage: www.elsevier.com/locate/scitotenv

Microplastics in bulk atmospheric deposition along the coastal region of Victoria Land, Antarctica

Silvia Illuminati [a,*], Valentina Notarstefano [a,*], Chiara Tinari [a], Matteo Fanelli [a], Federico Girolametti [a], Behixhe Ajdini [a], C. Scarchilli [b], V. Ciardini [b], A. Iaccarino [b], E. Giorgini [a], A. Annibaldi [a,1], C. Truzzi [a,1]

[a] Department of Life and Environmental Sciences, Università Politecnica delle Marche, Ancona, Italy
[b] Laboratory of Observations and Measures for the environment and climate, ENEA, Roma, Italy

HIGHLIGHTS

- Atmospheric deposition of about 1.7 MP m^{-2} d^{-1} was measured in Victoria Land
- Fragments were the most common morphotype identified.
- PP and PE were the dominant polymer types.
- Coastal sites were strongly affected by local anthropogenic activities.

GRAPHICAL ABSTRACT

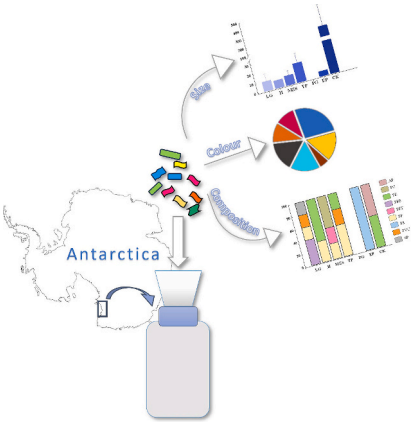

ARTICLE INFO

Editor: Philip Hopke

Keywords:
Microplastics
Bulk sampler
Raman Microspectroscopy
Air-mass backtrajectories
Antarctica

ABSTRACT

The increasing global concern over microplastic pollution has driven a surge in research efforts aimed at detecting microplastics across various ecosystems. Airborne microplastics (MPs) have been identified in remote environments worldwide, including Antarctica. However, data on bulk atmospheric deposition remain scarce. From January to December 2020, atmospheric deposition was directly collected using passive samplers placed in eight sites across Victoria Land. Using Raman Microspectroscopy, MPs were identified in six out of the seven samples collected (one sample was lost due to the extreme weather conditions). The average daily MP deposition for Victoria Land was 1.7 ± 1.1 MPs m^{-2} d^{-1}, with values ranging from 0.76 to 3.44 MPs m^{-2} d^{-1}. The majority (53 %) of MPs found in the atmospheric deposition were in the size class of 5–10 μm, and the main shape of MPs was fragments (95 %). The predominant plastic type was polypropylene (31 %), followed by polyethylene (19 %) and polycarbonate (12 %). Polystyrene, polyester, styrene and polyethylene terephthalate each accounted for

* Corresponding authors.
E-mail addresses: s.illuminati@staff.univpm.it (S. Illuminati), v.notarstefano@staff.univpm.it (V. Notarstefano).
[1] These authors contributed equally as co-last.

https://doi.org/10.1016/j.scitotenv.2024.175221
Received 20 December 2023; Received in revised form 28 June 2024; Accepted 31 July 2024
Available online 2 August 2024

~6 %. Microplastics identified in the coastal sites may have local origins, potentially associated with scientific activities at research stations. Conversely, a backward trajectories analysis suggested a potential contribution of atmospheric transport to microplastic deposition at Larsen Glacier and Tourmaline Plateau, the two most remote sites of the study area, where the highest MP concentrations were detected. Our findings present the first evidence of microplastics in the Antarctic atmospheric deposition directly collected via passive samplers, highlighting the need for continued monitoring and research to assess the environmental impact of MPs, particularly in sensitive and remote ecosystems like Antarctica.

1. Introduction

Plastic pollution is a pressing global environmental issue, affecting marine life, biodiversity, ecosystems, and economies. Over 8 million tons of plastic enter the oceans annually, with projections suggesting 33 billion tons produced by 2050 if current consumption rates persist (Geyer et al., 2017). Plastic breaks down into microplastics, plastic pieces with a diameter < 5 mm, through various processes, like biotic and abiotic degradation, photooxidation, and physical abrasion. These microplastics stem from diverse sources, either intentionally produced (primary MPs such as microbeads in cosmetics, personal care products, textiles) or resulting from the environmental degradation of larger plastic fragments (Cole et al., 2011).

It is well-known that MPs enter the environment at all stages of plastic production, from producers to waste management, following the "plastic cycle" – the continuous movement of plastics among different biotic and abiotic compartments (Bank and Hansson, 2019). The most prevalent plastic types, like polypropylene (PP), low- and high-density polyethylene (LDPE, HDPE), polyvinyl chloride (PVC), polyurethane (PUR), polyethylene terephthalate (PET), polyester (PES), and polystyrene (PS), are widely used in packaging, construction, textiles, microbead and microexfoliated personal-care products (PlasticsEurope 2019; Geyer et al., 2017; Wu and Yang, 2017). Environmental matrices often reflect this production pattern, with PP, PE, PET, PES, and nylon being the most common microplastic constituents (Cole et al., 2011). Microplastics are not inert; they react with atmospheric oxidants like oxygen, ozone, hydroxyl radicals, and nitrogen oxides (Bianco et al., 2020; Vicente et al., 2009), producing harmful organic compounds. These compounds pose risks to ecosystems and can accumulate in aquatic organisms, causing internal injuries, and behavioral changes (Cole et al., 2011). Recent discoveries include MPs in human tissues like the intestine, placenta, breast milk, urine, and semen (Schwabl et al., 2019; Ragusa et al., 2021, 2022; Pironti et al., 2023; Montano et al., 2023). Additionally, MPs can act as carriers of chemicals (potentially toxic metals, polycyclic aromatic hydrocarbon, additives) and biota (invasive species, pathogens), thus increasing the dispersal and transport processes in the environment (Cole et al., 2011).

During the past decade, an increasing number of studies have highlighted the pivotal role of atmospheric transport and deposition processes in MP occurrence in areas far away from emission sources (Brahney et al., 2020; Evangeliou et al., 2020; Zhang et al., 2021; Allen et al. 2019; González-Pleiter et al., 2019; Cai et al., 2017; Dris et al., 2016). Atmospheric deposition (e.g., dry deposition of particles, wet deposition with rain, and snow) is the main process through which atmospheric pollutants are removed from the atmosphere and transferred to terrestrial and aquatic ecosystems (Amodio et al., 2014). A Study by Allen et al. (2019) have implicated atmospheric transport in the long-range dispersion of MPs, particularly those sized between 25 and 300 μm. Notably, Evangeliou et al. (2020) assessed the likelihood of road traffic-emitted MPs reaching remote regions, estimating varying transport efficiencies across different areas, such as the Atlantic Ocean, South China, the Pacific Ocean, and the Arctic.

Like the Arctic, Antarctica is regarded as a pristine environment owing to its remoteness from continents, where local sources such as wind-blown dust, biogenic emissions from soils and vegetation, or anthropogenic emissions prevail. Research on MPs in Antarctica is relatively recent, with most studies focused on the marine environment. Microplastics and microfibres were found in marine surface waters of the Southern Ocean (Isobe et al., 2017; Suaria et al., 2020; Waller et al., 2017), as well as in marine sediments, marine and terrestrial organisms (zooplankton, Antarctic krill, collembola, penguins, seabirds) (Cunningham et al., 2020, Absher et al., 2019, Sfriso et al., 2020, Bergami et al., 2020a, 2020b, Bessa et al., 2019, Ibañez et al., 2020), and recently, also in the freshwaters of an Antarctic Specially Protected Area (ASPA) on Livingston Island (González-Pleiter et al., 2020). Despite the identification of airborne MPs in remote areas (Allen et al. 2019; Ambrosini et al., 2019; Brahney et al., 2020; Zhang et al., 2021), data on Antarctic atmospheric deposition are very scarce. The only available studies on airborne MPs in Antarctica are those of Aves et al. (2022) and González-Pleiter et al. (2021). Aves et al. (2022) collected fresh surface snow samples from different sites across the Ross Island region, while González-Pleiter et al. (2021) investigated plastic occurrence on two ice surfaces (one area around Uruguay Lake and another one around Ionosferico Lake), constituting part of the ablation zone of Collins Glacier (King George Island, Antarctica).

Under the Italian Antarctic Project PNRA 2015/AZ3.01, the chemical composition and spatial distribution of atmospheric aerosol were studied in Victoria Land (Antarctica) during winter 2020. Atmospheric deposition was directly collected at eight sites using passive bulk samplers to investigate the abundance, characteristics, and potential sources of microplastics, also through the evaluation of meteorological parameters' influence and air mass backtrajectories analysis.

2. Materials and methods

2.1. Study area

During the XXXV Italian Expedition in Antarctica (austral winter 2020), passive bulk samplers were installed at eight sites (Fig. 1) throughout the Victoria Land region. Each site is provided with an Automatic Weather Station (AWS) of the Italian Antarctic Meteo-Climatological Observatory (IAMCO) as part of the National Research Program in Antarctica (PNRA). Unfortunately, as has occurred during the last four expeditions, including the winter of 2020, the bulk sampler installed at Mario Zucchelli Station (MZS) was lost due to katabatic wind events, which are common during winters along the Antarctic coasts.

Victoria Land is a region of the Antarctic continent that borders the western side of the Ross Sea and the Ross Ice Shelf. It extends southward from about 70°30′ S to 78°00′ S and westward from the Ross Sea to the edge of the Antarctic Plateau. Positioned at 15 m above sea level (a.s.l.) on a granite promontory in Terra Nova Bay, MZS (74°42′S, 164°07′E) serves as a strategic logistic hub for both national and international research stations in Antarctica. Since 1985, the Station has been operational only during the austral summer, supporting all research activities of the PNRA and hosting an average of 300 logistical and scientific personnel annually during the opening period (about four months). Near MZS are the German Station Gondwana (~ 6 km to the north), which operates only during the summer, though not every year, and the South-Korean Jan Bogo Station (~ 8 km to the north), which remains operational year-round. During the study period, the AWS installed at MZS recorded several katabatic wind events with average wind speeds of 20–30 m s^{-1} and gusts up to 60 m s^{-1} (data not reported). Faraglione

Camp (74°43′S, 164°6.9′E), the first sampling site, is located about 3 km south of MZS. Details of this site have been reported elsewhere (Bertinetti et al., 2022; Vagnoni et al., 2021). Inexpressible Island (74°54′S, 163°39′E) lies about 30 km south of MZS. Positioned at the edge of the Nansen Ice Shelf, this small rocky island stands at the confluence of two major glaciers, Reeves and Priestley. It is largely free of ice due to strong katabatic winds blowing from inland. The island is notable for its penguin rookeries and south polar skuas nesting sites. Larsen Glacier (74°57′S, 161°46′E), about 70 km southwest of MZS, spans 5 km in width and extends approximately 40 km in length. It flows southeastward along the southern slopes of Mounts Larsen, De Gerlache, and Crummer before merging with the Reeves Glacier on the Nansen Ice Sheet. Further north, Edmonson Point (74°20′S, 165°08′E) lies in Wood Bay along the western coast of the Ross Sea (Fig. 1) on the slope of Mount Melbourne. Designated as an Antarctic Specially Protected Area (or ASPA), this site hosts Adelie penguin colonies and skua nests. Cape King (73°35′S, 166°37′E) stands as a promontory (~ 160 m a.s.l.) forming the seaward end of the rocky west wall of Wylde Glacier as it meets Lady Newnes Bay in the Ross Sea. Lastly, the Tourmaline Plateau and Priestley Glacier are situated west of MZS. Tourmaline Plateau (74°10′S, 163°27′E) is an ice-covered plateau within the central portion of the Deep Freeze Range, bordered by the Howard Peaks and a series of north-south trending peaks and ridges from Mount Levick. Priestley Glacier (74°10′ S, 162°53′ E) originates from the Victoria Land Plateau, flows for about 96 km, and joins the Nansen Ice Sheet after flowing through a 7-km wide valley.

The AWSs at the various sampling sites recorded hourly values of the principal meteorological parameters (air temperature, relative humidity, ambient pressure, wind speed and direction) from January to December 2020. Details of the meteorological conditions of each sampling site together with their corresponding wind rose are provided in Supplementary Material (Text S1; Figs. S1–6). Here is a brief description of the average data recorded by the AWS during the sampling period. Temperature, atmospheric pressure and relative humidity showed values of −22 ± 9 °C, 906 ± 62°hPa and 57 ± 10 %, respectively. Wind speeds averaged 8.5 ± 5.4 ms^{-1}, peaking at ~20 ms^{-1} at Priestley Glacier in July. Winds reached up to ~25–30 ms^{-1} from March to November in sites facing Terra Nova Bay, with prevailing wind directions varying across locations. Cape King experienced frequent calm episodes, with an average wind speed of ~2 ms^{-1}. Meteorological data for Edmonson Point were unavailable due to technical issues. Unfortunately, information regarding snow precipitation was not available as the relative sensor was installed one year after the current campaign. However, the AWS at Larsen Glacier was equipped with a snow accumulation sensor. A graph illustrating the average snow accumulation (measured as height from the snow ground) at Larsen Glacier throughout the sampling period has been included in the Supplementary Material (Fig. S7). It can be noted that the snow accumulation was generally low, except for a significant snowfall event on September 1st 2020, where it reached approximately 1 m in height.

2.2. Field collection and sample treatment

From January to December 2020, a total of seven atmospheric deposition samples were collected using bulk samplers. Each sampler, consisting of a PE funnel connected to a bottle of the same material, was placed inside a 1.5 m long PVC pipe, following the approach of Klein and Fischer (2019) or Allen et al. (2019). The PVC pipes were specifically modified to ensure the bulk funnel's position at 1.5 m above the ground. They served as protecting housings, shielding the samplers from UV radiation and abrasion, thus preventing the collection of re-suspended soil particles or drifting snow. Each bulk sampler, housed within its PVC pipe, was anchored to the trellis of the respective AWS present at the sampling site. Ideally, samples would have been collected monthly. However, due to the winter closure of MZS, the sampling strategy extended over approximately nine to ten months per sample (see Table 1 for the exact sampling days). Therefore, one sample was collected for each sampling site, except for Mario Zucchelli Station where the bulk sampler was lost due to the extreme winter weather conditions. To assess background contamination, sample blanks ("field blanks") were also collected in the field at the beginning and the end of the sampling campaign (two field blanks at the Larsen Glacier and another two at the Mario Zucchelli Station). These were obtained by placing the bulk sampler into the PVC pipe for 20–30 min and then treated as the deposition samples. The bulk samplers containing the deposition samples and field blanks were stored at −20 °C before being transferred to the Italian laboratories. Once in Italy, bulk samples were thawed at room

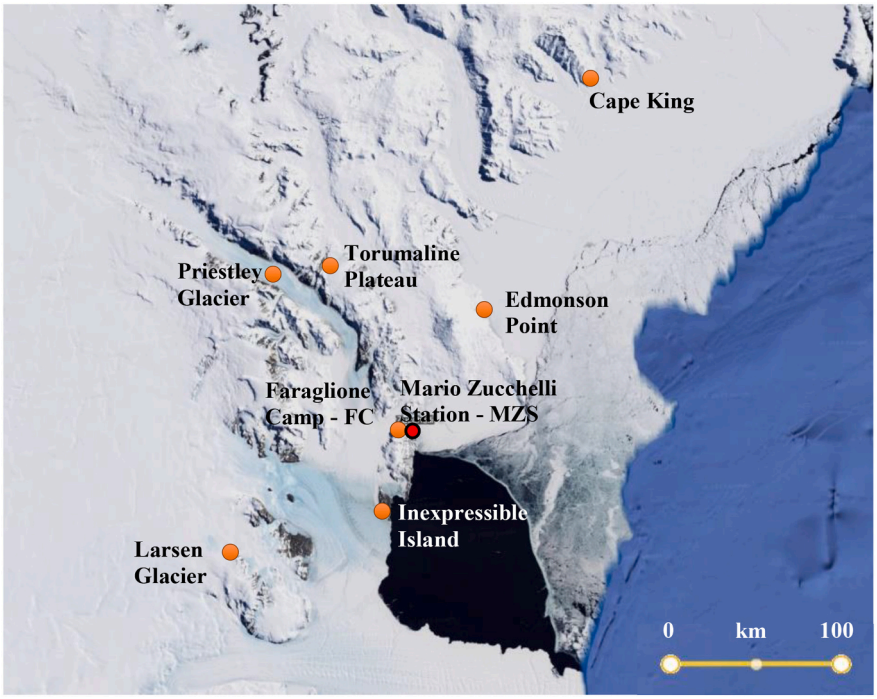

Fig. 1. Map of the Victoria Land region, showing the sampling sites and the position of the Italian Antarctic Station "Mario Zucchelli" (MZ). Map data ©2023 Google.

Table 1
Atmospheric microplastic (MP) deposition (m^{-2} d^{-1}) in the study area. The distance of each sampling site from the Mario Zucchelli Station and the sampling period are also reported.

Sampling site	Geographical Coordinates	Distance from MZS, (km)	Altitude (m, asl[a])	Sampling period	Total flux (MPs m^{-2} d^{-1})
Larsen Glacier	74°57'S 161°46'E	80	1250	07/01/2020 – 10/12/2020	3.44 ± 0.25
Inexpressible Island	74°54'S 163°39'E	30	20	07/01/2020 – 29/11/2020	2.13 ± 0.15
Faraglione Camp-MZS	74°43'S 164°6.9'E	3	60	20/01/2020 – 20/12/2020	2.78 ± 0.20
Tourmaline Plateau	74°10'S 163°27'E	50	1621	06/01/2020 – 18/11/2020	2.93 ± 0.21
Priestley Glacier	74°10' S 162°53' E	80	880	06/01/2020 – 27/11/2020	n.a.
Edmonson Point	74°20'S 165°08'E	50	30	18/01/2020 – 17/11/2020	0.76 ± 0.05
Cape King	73°35'S 166°37'E	159	160	20/01/2020 – 05/12/2020	1.45 ± 0.10

[a] asl, above the sea level.

temperature in a Clean Room (Class 5, ISO 14644-1 or Class 100 according to US Fed. Std. 209e) and vacuum-filtered through 47 mm glass fibre membrane (with pore diameter of 0.7 μm, Whatman, GF/B GE Healthcare Life Sciences, Buckinghamshire, UK) with a borosilicate glass filtration system (Carlo Erba, Italy). When no wet deposition was collected, 500 mL of ultrapure pre-filtered water (Milli-Q, Merck-Millipore, Darmstadt, Germany) was added to re-suspend any particles attached to the inner surface of the bulk. The solutions obtained after filtration were stored in LDPE 500-mL bottles at −20 °C for future analysis. An aliquot (1/8) of this filter (referred to as MF_0 for simplicity) was cut by stainless steel scissors previously decontaminated with ultrapure pre-filtered water and then transferred into a borosilicate glass beaker and treated with 15 mL of 30 % superpure pre-filtered H_2O_2 (Carlo Erba, Italy). It was then covered with a glass lid and placed in a static heat oven (BINDER GmbH, mod. ED 115, Tuttlingen, Germany) at +60 °C for 24 h. The next day, the H_2O_2 digestion solution was filtered onto a 0.7-μm glass fibre filter (MF_1). The MF_0 filter with the remaining material was dried under the laminar flow areas of the Clean Room at room temperature. After the H_2O_2 digestion, MPs were extracted from MF_0 using the dry ultrasonic methodology (DU-32 Digital ultrasonic cleaner, ArgoLab, Modena Italy) as applied by Faraji et al. (2018), followed by gentle sweeping with a decontaminated brush. The MF_0 was then removed from the glass beaker and dried in the Clean Room at room temperature. After the extraction, the MPs remaining in the beaker were resuspended in 10 mL of pre-filtered Milli-Q water. The aqueous solution of MPs was vacuum-filtered onto a 0.7-μm glass fibre membrane (MF_2). This final filter was dried under laminar flow at room temperature. All the glass fibre membranes (MF_0, MF_1, and MF_2) were stored in glass Petri dishes at room temperature until RMS analysis.

2.3. Detection and identification of MPs by RMS

Raman Microspectroscopy analysis was performed by using an XploRA Nano Raman Microspectrometer (Horiba Scientific) at the Advanced Research Instrumentation (ARI) Laboratory of Università Politecnica delle Marche (Ancona, Italy). All filter membranes (MF_0, MF_1 and MF_2), including those related to the field and procedural blanks, were examined by visible light using a × 10 objective (Olympus MPLAN10×/0.25). By using a × 100 objective (Olympus MPLAN100×/0.90), the detected MPs were morphologically characterized and then directly analysed on the filter by RMS (spectral range 200–1800 cm^{-1}, 532 nm or 785 nm laser diode, 600 lines per mm grating). A 16-bit dynamic range Peltier-cooled CCD detector was used for spectra dispersion; the 520.7 cm^{-1} line of silicon was employed to calibrate the spectrometer before spectral acquisition. Raw Raman spectra were subjected to polynomial baseline correction and vector normalisation, to reduce noise and enhance spectrum quality (Labspec 6 software, Horiba Scientific). To identify the polymer matrix of the detected particles, the collected Raman spectra were compared with spectral libraries of polymers and pigments obtained by measuring standard polymers/compounds (KnowItAll software, John Wiley & Sons, Inc., Hoboken, NJ, USA) (Dong et al., 2020; "SLOPP Library of Microplastics,", n.d.). Similarities of more than 80 of the Hit Quality Index (HQI) were accepted. No MPs were identified on filter MF_0 nor on filter MF_1 following the extraction procedure for all the bulk samples and field blanks collected.

2.4. Quality assurance and control (QA/QC)

Quality control is challenging when dealing with Antarctic samples, especially in the study of microplastics. To address this challenge, a plastic-free protocol aimed at preventing microplastic contamination was implemented during sample treatment and analysis. As mentioned earlier, two sets of field blanks were collected at the beginning and end of the field campaign. These field blanks were subjected to the same procedure as the deposition samples. Additionally, a procedural blank was prepared at the beginning of each day of analysis, following the exact procedure used for the samples but without adding bulk samples. The filters derived from both field and procedural blanks were inspected and treated using the same approach as the samples.

Clothing was closely monitored throughout the entire process. As emphasized by Aves et al. (2022), the Italian Antarctic Programme provides essential clothing and field gear to staff and scientific personnel. Some of this gear is mandatory for outdoor work at research stations. Aves et al. (2022) catalogued the composition of the entire field gear provided by the New Zealand National Antarctic Programme (including base layers, mid-layers, shoes, boot liners, gloves, bags, hats, and accessories) to determine potential local sources of fibrous material found into snow samples from the Ross Island region. During sample collection, our researchers stood downwind of the sample to avoid contamination from clothing. In Italy, all sample treatment steps were carried out under the laminar flow areas of the Clean Room. All metal, steel and glass materials were thoroughly cleaned with previously filtered Milli-Q water and acetone before analysis. Surfaces were cleaned with ethanol (70 %) before sample pre-treatment and RMS analysis. During laboratory manipulation, researchers wore 100 % monofilament polyester laboratory coats with antistatic carbon fibres to prevent particles released from the human body (skin, hairs, and hair). Single-use nitrile gloves and face masks were also worn throughout sample manipulation and treatment. No fragments or fibres were detected in the field blanks. Additionally, none of the microplastics identified exhibited the same color as that of the bulk collectors (white) and the PVC pipe (grey).

2.5. Data processing and statistical analysis

The deposition of atmospheric microplastics (AD_{MP}) in collected

samples was calculated following the equations reported by Allen et al. (2019). The count of MPs in each MF_2 (MPs m^{-2}) as extracted from each 1/8 aliquot of the original filter, provides an indication of the MP quantity per sample. Nevertheless, it has to be pointed out that extrapolating from subsampled filters does not give a precise MP count, but rather an estimation of MPs per filter (and consequently per sample). Ideally, all the particles should be counted and confirmed by RMS, but due to analysis constraints and filter sample availability, a complete analysis of the filter was not possible. The calculation of the atmospheric deposition (MP m^{-2} d^{-1}) was given as MP counts in each filter MF_2, scaled using the known filter, bulk sampler area and the sampling period. The following equations of Allen et al. (2019) were applied:

$$MP = \left(X \bullet \frac{Y}{y}\right) - \varepsilon \quad (1)$$

where MP = the total MP count per filter; X = total number of MPs identified in MF_2, corresponding to the 1/8 of the original filter as obtained after the deposition filtration (MF_0); Y = the total original filter area (i.e. $\pi r^2 = 3.14 \bullet (0.024)^2 = 0.0017$ m^2); y = the sample area MF_0, corresponding to the 1/8 of the original filter as obtained after the filtration of the atmospheric deposition (i.e. $y = Y \div 8 = 0.0017 \div 8 = 0.00022$ m^2), and ε = the sampling error, the number of MP particles found on the blank samples and scaled up to the 1/8 portion of the original filter.

$$AD_{MP} = \frac{MP}{a \times t} \quad (2)$$

where AD_{MP} = atmospheric deposition reported in MP m^{-2} d^{-1}; MP = total MP counted per filter and computed as in Eq.1; a is the collection area (i.e., funnel area) in m^2; t = the sampling period expressed in days. Reporting data as microplastics per square metre is generally accepted in literature as a method for comparing results from multiple studies (Amodio et al., 2014). In the calculation of daily atmospheric deposition, a collection area, a, of 0.034 ± 0.003 m^2 was considered as obtained from the average of the funnel areas of each bulk sampler.

Given the limited dataset ($n = 6$), Spearman's non-parametric correlation test was applied to identify the relationship between size, colors, MP atmospheric deposition, and meteorological parameters. For statistical purposes, MPs were subdivided into two color groups: the dark group including all the black, brown, and blue particles, and the light group with all light blue, magenta, orange, and yellow MPs. Meteorological parameters were averaged over the entire sampling period (i.e. nine-ten months). Additionally, the average wind directions were calculated by averaging the north–south (NSW) and east–west (EWW) components of the wind. The statistical analysis was carried out using Statistica package (StatSoft; vers. 8.0) and the differences were considered statistically significant at $p < 0.05$.

2.6. Air-mass backtrajectories

To understand the potential sources of atmospheric MPs, the air mass transport pathways over the study sites were characterized using back trajectories generated by the Hybrid Single-Particle Lagrangian Integrated Trajectories (HYSPLIT) model v.5.0.0, developed by NOAA (National Oceanic and Atmospheric Administration) and Australia's Bureau of Meteorology (Rolph et al., 2017; Stein et al., 2015). Back-trajectories (TJs) were calculated for the arrival heights of 500 m a.g.l. (above the ground level) at the site from January 10, 2020, to December 10, 2020. The ERA5 reanalysis, archived as a meteorological gridded dataset, initialized the HYSPLIT model. The ERA5 was provided by the European Centre for Medium-range Weather Forecasts (ECMWF; Hersbach et al., 2020). The dataset is available on 37 pressure levels with a regular spatial grid of 0.25° x 0.25° at hourly temporal sampling. Due to computational constraints, we utilized ERA5 parameters on a spatial grid of 0.5° x 0.5° every three hours and 24 pressure levels, following the methodology of Becagli et al. (2022). We computed height TJs per day, ending above the site every three hours, and each trajectory was calculated up to 168 h back in time. This threshold was selected based on a recent study by Brahney et al. (2021), which estimated the residence time of microplastics in the atmosphere to vary between 1 and 156 h. Therefore, as also applied by Aves et al. (2022), we ran back trajectories for 168 h to show the full range of possible sources. After five days, the uncertainty associated with trajectories was estimated to be between 10 and 30 % of the travel distance (Scarchilli et al., 2011; Schlosser et al., 2008). Model precipitation at each studied site was evaluated by extracting the time series of the nearest model grid point for the ECMWF ERA5 (Hersbach et al., 2020) reanalysis total precipitation field. Wind speed data were directly measured at each site at 3 m above the ground by the AWS operated by IAMCO (www.climantartide.it) (Scarchilli et al., 2020).

The primary paths of air masses reaching each site were evaluated by dividing the southern hemisphere in a regular 0.5° x 1° mesh and counting the number of back trajectories spending at least one hour in each grid cell. To highlight the air mass pathway connected with katabatic winds or snowfall occurrences, a similar counting procedure was applied selecting back trajectories associated with events during which wind speed or snowfall at the site exceeded a certain threshold. The 50th percentile of the wind speed or precipitation data distribution for each site during the studied period was used as threshold.

3. Results and discussion

3.1. Atmospheric deposition of microplastics in the Victoria Land

Microplastics were detected in six out of the seven bulk deposition samples collected during the austral winter 2020 in Victoria Land. No particles or fibres were detected in the deposition collected at Priestley Glacier. A total of 136 particles were estimated as microplastics using RMS across the six field samples. (Fig. 2). Images of microplastic particles, along with their polymer type and color, collected during the sampling period, are included as examples in Supplementary Material (Table S1).

The daily MP deposition recorded in the Victoria Land showed an average ± standard deviation of 1.7 ± 1.1 MPs m^{-2} d^{-1}, with values ranging from 0.76 ± 0.05 MPs m^{-2} d^{-1} at Edmonson Point, to 3.44 ± 0.25 MPs m^{-2} d^{-1} at Larsen Glacier (Table 1). Microplastic deposition in the Victoria Land followed the order (excluding Priestley Glacier): Larsen Glacier > Tourmaline Plateau > Faraglione Camp > Inexpressible Island > Cape King > Edmonson Point. Although numerous studies have reported significant MP pollution in the marine environment, the presence of atmospheric microplastics in Antarctica is a recent discovery (González-Pleiter et al., 2021; Aves et al., 2022) and, to our knowledge, no study reports the detection of MPs in Antarctic atmospheric deposition, directly collected. Our average daily atmospheric deposition was one order of magnitude higher than the dry depositional rate estimated by González-Pleiter et al. (2021) in the ablation area of Collins Glacier (King George Island, Antarctica). Table 2 shows a summary of available results from worldwide research on microplastic atmospheric deposition. It is evident that data on MP atmospheric deposition vary significantly from one study to another, with values ranging from 100 to 1000 particles $m^{-2}d^{-1}$ in highly urbanized cities of Europe and Asia (Cai et al., 2017; Dris et al., 2016; Klein and Fischer, 2019; Szewc et al., 2021; Wright et al., 2020) to 0–600 particles $m^{-2}d^{-1}$ in rural and remote areas of Europe, the USA, Canada, Iran, and Vietnam (Abbasi et al., 2019; Allen et al., 2019; Brahney et al., 2020; Roblin et al., 2020; Truong et al., 2021; Welsh et al., 2022). This high variability cannot solely be attributed to differences in site environmental features but it is likely also due to differences in analytical procedures. It is noteworthy that at the time of our sampling campaign, no standard operating procedure had been released for atmospheric MP analysis. Recently, a novel glass/metallic standardized sampling equipment for atmospheric deposition was

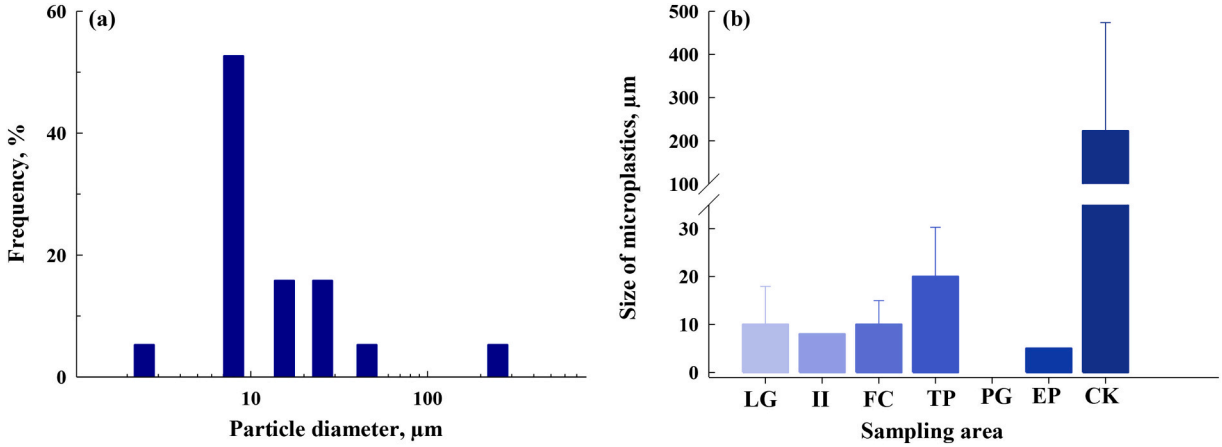

Fig. 2. Dimensional characteristics of microplastics in all the collected atmospheric depositions: unimodal distribution of identified microplastics (2a) and spatial distribution of size-range MPs in the study area (2b). LG = Larsen Glacier; II = Inexpressible Island; FC = Faraglione Camp; TP = Tourmaline Plateau; PG = Priestley Glacier; EP = Edmonson Point; CK = Cape King.

Table 2
Characteristics of microplastics (MP) in atmospheric depositions in remote and urban areas.

Site	Site type	Sampling period (months)	Type of collector	Sampling height [a] (m)	Shape (%)	Size (µm)	Polymer type	Total flux (MPs m^{-2} d^{-1})	Source
Victoria Land, Antarctica	Remote	9–10	Bulk	1.5	Fragments (95 %) Fibres (5 %)	5–400	AP, PS, PC, PET, PE, PES, PP, PVC, SP	1.7 ± 1.1	This study
King George Island, Antarctica	Remote	12 h for 2 days	12 squares of ice surface	N/A	Fragments	L: 2292–12,628 W: 501–11,334	EPS	0.08–0.17	González-Pleiter et al., 2021
Ross Island	Remote	Late 2019	Surface snow	N/A	Fibres, fragments, films	50–3500	PET, PA, PVC, PE, ALK, PP, PTFE	29 particles L^{-1}	Aves et al., 2022
Pyrenees mountains, France	Remote	5	Bulk	N/A	Fragments (68 %) Films (20 %) Fibres (12 %)	<50 50–150 150–300	PS, PE, PP, PVC, PET	249 73 44	Allen et al., 2019
Muskoka-Haliburton, Canada	Remote	13	Wet-only Bulk	1.7	Fibres, particles	20–5000	PA, PET	7 (4–9)	Welsh et al., 2022
Western protected areas, USA	Remote	Fall 2017 through the summer 2019	Wet, dry	N/A	Fibres, particles	N/A	PE, PP, PVA, AP	132 ± 6	Brahney et al., 2020
Ho Chi Minh City, Vietnam	Rural Urban Landfill	12	Dry, wet	2	Fibres, fragments	300–5000	PE, PP, PS, cellulose	256 374 230	Truong et al., 2021
London, England	Urban	1	Bulk	on the roof top (~50 m)	Fibres, fragments, films, granules, foams	5–75	PAN, PET, PA	712 ± 167	Wright et al., 2020
Paris, France	Urban Suburban	12 6	Bulk	on the roof top	Fibres	50–1400	PE, PP, PS	110 ± 96 53 ± 38	Dris et al., 2016
Ireland	Rural Remote	12	Wet-only Bulk	N/A N/A	Fibre	40–19,750	PET, PAN, PE, PP	60–77 100 ± 52	Roblin et al., 2020
Hamburg, Germany	Urban Forest Rural	2	Bulk	1.0	Fragments (95 %), fibres (5 %)	60–300	PE, EVAC, PTFE, PVA, synthetic fibres	136–261 331–512 343	Klein and Fischer, 2019
Shiraz and Mount Derak, Iran	Urban Remote	12	Dry, wet	3–4	Fibres, particles	100–1000	PP, PS, PE	63.6 12.2	Abbasi and Turner, 2021
Donguuan, China	Urban	3	Bulk	15	Fibres, films, foams, fragments	200–700	PE, PP, PS, cellulose	175–313	Cai et al., 2017

developed by the Norwegian Institute for Air Research (NILU) and was used for the first time by Allen et al. (2019). Although not standardized, our device has the same sampling area as the NILU (0.034 m^2) and other collectors used in several studies (Klein and Fischer, 2019; Welsh et al., 2022; Roblin et al., 2020). Atmospheric deposition samplers were installed at different heights, such as at 15 m height in Cai et al. (2017), on the rooftop (at ~50 m above ground level, agl) in Dris et al. (2016), at ~1.7 m above ground in Welsh et al. (2022), at 1 m in Klein and Fischer (2019) or at 1.5 m agl as in our study. It should be emphasized that while the snow accumulation in our sampling sites remains low (below the 1.5 m of bulk opening distance from the ground), as indicated by the sensor installed at the Larsen Glacier AWS, the potential influence of snowdrift

cannot be excluded. This is because our system is not specifically designed to sample precise volumes of precipitation. Additionally, detection methodologies for quantifying MPs varied among studies. Dris et al. (2016), Cai et al. (2017) and Szewc et al. (2021) applied visual inspection followed by μFTIR verification. Klein and Fischer (2019) and Allen et al. (2019) pre-identified MPs via fluorescence microscopy and then utilized RMS for verification. Similar to Roblin et al. (2020) and Welsh et al. (2022), we conducted visual inspection using visible light and applied the RMS for verification.

3.2. Characteristics of microplastics

In the Victoria Land, atmospheric MP deposition mainly consisted of fragments, accounting for about 95 % of the total MPs, with fibres comprising the remaining 5 %. No films or beads were detected. Fibres were only present at Cape King, the northernmost site, (Table S1), while fragments were widespread across all study sites. Our findings align with the observation that fragments tend to be abundant in remote environments, with the exception of Hamburg (Klein and Fischer, 2019), whereas fibres are more prevalent in urban and suburban areas. This disparity could be attributed to the size difference, as fragments are usually smaller than fibres, and can be easily suspended and transported by winds. Additionally, larger MPs may undergo mechanical processes during atmospheric transport, degrading into smaller particles. Recent studies (Tatsii et al., 2024) show that large fibres (1 mm in length) emitted in populated areas may have a lower settling velocity, allowing them to reach extremely remote regions like the Arctic.

Nonetheless, studies in Antarctica have revealed a varied distribution of MPs, depending on the sample type. For instance, fragments were prevalent in seawater (Cincinelli et al., 2017) and krill (Ibañez et al., 2020), while fibres dominate surface snow in Ross Island (Aves et al., 2022) and marine sediments inTerra Nova Bay (Munari et al., 2017).

The modal diameter of the observed fragments fell in the class 5–10 μm (mean ± SD, 8.7 ± 1.5 μm, Fig. 2a), with the thinnest and thickest fragments measuring around 5 and 45 μm, respectively. Fibrous microplastics exhibited higher diameter values, with an average length of 400 μm. Tourmaline Plateau displayed the highest size variability, with MPs ranging from 7 to 30 μm (median ± SD, 20 ± 10 μm, Fig. 2b), followed by Larsen Glacier and Faraglione Camp (10 ± 8 μm, and 10 ± 5 μm, respectively, Fig. 2b). The wide size range of MPs observed at Cape King is attributed to the presence of fibres with an average length of 400 μm. The size distribution of MPs in Victoria Land agreed with studies in other remote or rural areas worldwide, like the Ross Island (Aves et al., 2022), the Southern Ocean (Isobe et al., 2017), in the Pyrenees (Allen et al., 2019), in Arctic snow (Bergmann et al., 2019), in rural area of Ireland (Roblin et al., 2020), in protected areas of the USA (Brahney et al., 2020) or in Alpine glaciers (Ambrosini et al., 2019).

Fig. 3 shows the principal colors of all detected MPs both (a) in the Victoria Land and (b) at each sampling site. Seven main colors were recognized (Fig. 3a), with blue being the most prevalent (26 % of the total MPs). The remaining colors followed the order black ≅ light blue ≅ yellow > magenta ≅ orange > brown. Our findings are consistent with those of Aves et al. (2022), who identified dark-colored MPs (blue, black and navy) as the dominant colors in the surface snow of Ross Island. Dark-colored MPs were present in all the samples except at Tourmaline Plateau and Cape King where only light-colored MPs (yellow, light-blue, magenta) were identified (Fig. 3b). Larsen Glacier exhibited the highest concentrations of dark-colored MPs (accounting for the16% of the total MPs collected) with black being the predominant color (~40 % of all the MPs detected at Larsen Glacier, Fig. 3b). The presence of dark-colored MPs in Antarctic atmospheric deposition is a matter of concern, since once deposited onto snow or glacier, they can efficiently absorb solar radiation, accelerating the melting process (Evangeliou et al., 2020). Wang et al. (2020) and Liu et al. (2019a) have also noted that black MPs are dominant in megacity atmospheres, suggesting a potential input of MPs from anthropized areas via long-range transport processes. However, Abbasi et al. (2019) detected high concentrations of white-transparent MPs in industrial (70 %) and urban areas (53 %). Therefore, the MP color alone cannot be used as a parameter to assess sources of MPs in the remote region of the Victoria Land.

Raman MicroSpectroscopy identified nine polymer types: polycarbonate (PC), polyethylene, polyesters, polyethylene terephthalate, polypropylene, polystirene, polyvinyl chloride, styrene plastics (SP), acrylic polymers (Fig. 4a). The most prevalent polymer type detected was PP, accounting for ~30 % of the total MPs, followed by PE, PC, and PES (Fig. 4a). Larsen Glacier showed the highest polymer variability, with PES accounting for 40 % of the total MPs. PP dominated at the Tourmaline Plateau (~50 %), while PE was common at Cape King and Inexpressible Island (~50 % and 70 %, respectively). PC was prevalent at Faraglione Camp (~50 %), and PS was the sole polymer found at Edmonson Point (Fig. 4b). Studies around the Ross Sea region have shown significant variability in the MP distribution. Notably, Aves et al. (2022) reported predominantly PET fibres in McMurdo Sound surface snow. Similar results were reported by Liu et al. (2019b) in atmospheric samples over the West Pacific Ocean. In Artic snow, Bergmann et al. (2019) identified varnish, acrylates, and polymethyl methacrylate. Fragments principally made of acrylic, polyester, alkyl and

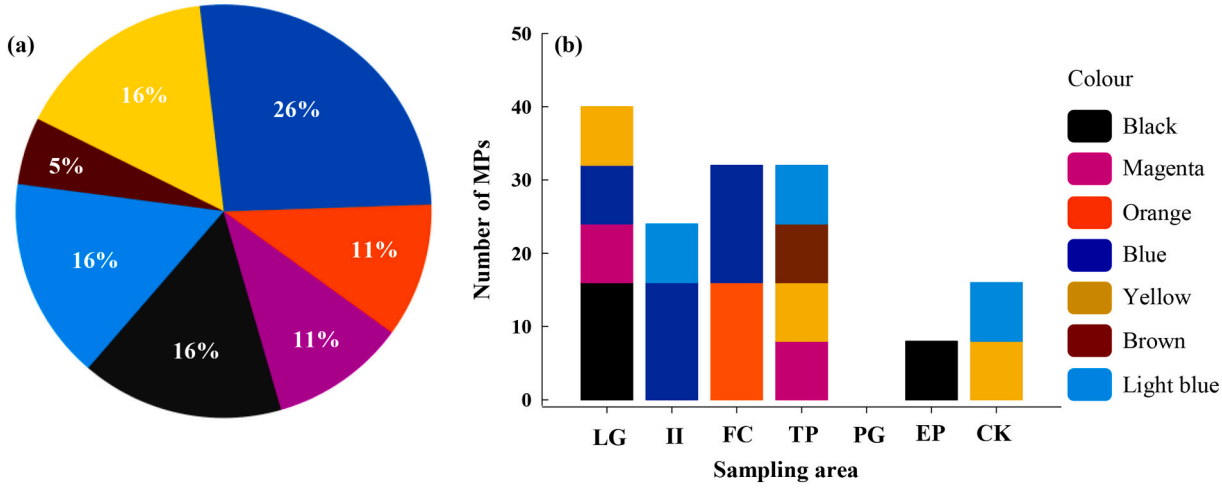

Fig. 3. Color of microplastics detected in all the atmospheric samples (a) and in the different sampling sites of the Victoria Land (b). LG = Larsen Glacier; II = Inexpressible Island; FC = Faraglione Camp; TP = Tourmaline Plateau; PG = Priestley Glacier; EP = Edmonson Point; CK = Cape King.

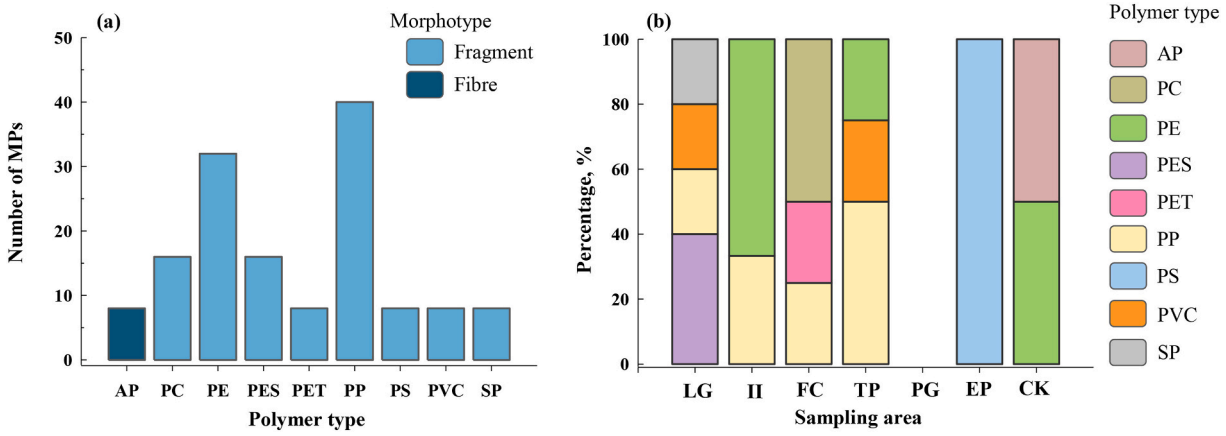

Fig. 4. The composition of microplastics in total atmospheric depositions. Polymer types of particles identified in all the atmospheric samples (a) and in the different sampling sites of the Victoria Land (b). AP = acrylic polymers; PS = polystirene; PC = polycarbonate; PET = polyethylene terephathalate; PE = polyethylene; SP = styrene plastics; PVC = polyvinyl chloride; PP = polypropyplene; PES = polyesters. LG = Larsen Glacier; II = Inexpressible Island; FC = Faraglione Camp; TP = Tourmaline Plateau; PG = Priestley Glacier; EP = Edmonson Point; CK = Cape King.

polyurethane were identified by Cunningham et al. (2020) in Antarctic deep-sea sediments, suggesting a possible contribution of varnish from ships, fishing vessels, or marine stations. Additionally, our results agreed with marine researches by Lacerda (2019), Cincinelli et al. (2017), Suaria et al. (2020), and Bessa et al. (2019), confirming the prevalence of PE and PP in seawater and marine organisms (e.g. gentoo penguins) within the Ross Sea and Southern Ocean.

3.3. Sources of microplastics

Atmospheric deposition varies significantly in space and time due to meteorological parameters (such as wind speed and relative humidity), airborne particle characteristics, and the specific study area (Amodio et al., 2014). Identifying the sources of Antarctic atmospheric MPs is challenging as they may originate locally or be transported over short or long distances (Aves et al., 2022).

Airborne MPs collected at Faraglione Camp, ~3 km from MZS, were primarily composed of PC, PET, and PP, materials commonly used in packaging, construction, scientific materials, and reusable products for daily activities in MZS (Fig. 4b). Unfortunately, the bulk collector placed within the MZS area was lost during the sampling campaign, preventing direct assessment of the station's impact. PP and PE were detected at Inexpressible Island, where MP deposition was comparable to MZS (Table 1). Despite being approximately 30 km from MZS, Inexpressible Island experiences high anthropogenic pressures due to its significance in Antarctic research. The construction of a Chinese Antarctic station on the island may also act as a local source of MPs in this area. The acrylic fibres found at Cape King may originate from Antarctic clothing, with logistical and scientific personnel typically wearing inner gloves made of black acrylic. Additionally, coastal sites may receive MPs from surface waters through sea spray emissions. Although the marine environment is generally considered a sink for MPs, recent studies have shown that some plastic particles can enter the atmosphere through marine aerosols (Allen et al., 2020). Antarctic coastal areas are subjected to significant inputs of sea-salt aerosols, particularly during the summer when pack ice melts, releasing particles, contaminants, viruses, and algae (Illuminati et al., 2020; Illuminati et al., 2016). Antarctic pack ice melts typically from mid-December to January, gradually replaced by new platelet and ice from late February. Therefore, any marine aerosol contribution likely occurred early in the sampling, possibly in January or February 2020, when the seawater surface was ice-free and exposed to wind. However, due to our study's low temporal resolution, we cannot measure this contribution. Finally, icebreakers, which transport personnel and supplies to research stations or retrieve them before winter sets in, frequently navigate the surface waters of Terra Nova Bay in January and February, introducing potential local sources of contamination.

Among our findings, the MP deposition at Larsen Glacier warrants particular attention. Situated at a high altitude (Table 1) near the initial margin of the Antarctic plateau (Scarchilli et al., 2010; Lee et al., 2021), Larsen Glacier showed higher MP deposition rates (~3.4 MPs m^{-2} d^{-1}, Table 1) compared to Faraglione Camp (~2.8 MPs m^{-2} d^{-1}, Table 1), despite experiencing less anthropogenic pressure. Airborne MPs at Larsen Glacier exhibited typical characteristics of "environmentally aged microplastics". Their surface morphology showed signs of roughness, including microcraks, pits, and broken edges (Table S1), resulting from aging processes, such as photooxidation, mechanical stress, and biodegradation, which plastic particles may undergo upon release into the environment. High MP deposition also occurred at the Tourmaline Plateau, where MPs exhibited quite different characteristics from those found at Larsen Glacier, indicating a potential local origin (Table S1).

The back-trajectories model applied for the entire sampling period (Fig. S8) showed that the air masses arriving at Larsen Glacier and Tourmaline Plateau followed paths delineated by Transantarctic Mountains, which divide the Antarctic continent and act as a barrier for air masses from the Antarctic Plateau (Fig. 5). Snow-fall associated TJs (i.e. those ending at the site during snowfall) were relatively few throughout the period (~15 %), with predominant paths over the Transantarctic Mountain (Fig. 5a, c). Conversely, considering TJs associated with stronger wind conditions (i.e. wind speed >10.3 ms^{-1}), typically originating from the plateau (i.e. katabatic wind) and with no snowfall at the sites, the contribution of transport from distant areas affecting MPs cannot be excluded (Fig. 5b, d). In fact, approximately 40 % of the air masses arriving at the sites were associated with katabatic winds, covering a broader area. The role of wind as a potential driver of MP transport and deposition from the Antarctic plateau was further highlighted by the results of Spearman's correlation test, which revealed a negative, statistically significant correlation between MP abundance and the east-west component of the wind (Table 3). A high correlation, though not significant, was also observed with wind speed. However, these data should be interpreted with caution due to the low dimensionality of the dataset (one sample per site) and low temporal resolution. Further research is necessary to better understand the role of wind on MP deposition in Antarctica. Several studies (Allen et al., 2019; Roblin et al., 2020; Szewc et al., 2021; Welsh et al., 2022; Wright et al., 2020) highlighted atmospheric transport's influence on particle deposition. For instance, Chen et al. (2012) showed that high wind speeds increase the dry deposition velocity of total suspended particles, promoting MP deposition. By applying a similar method as Allen et al.

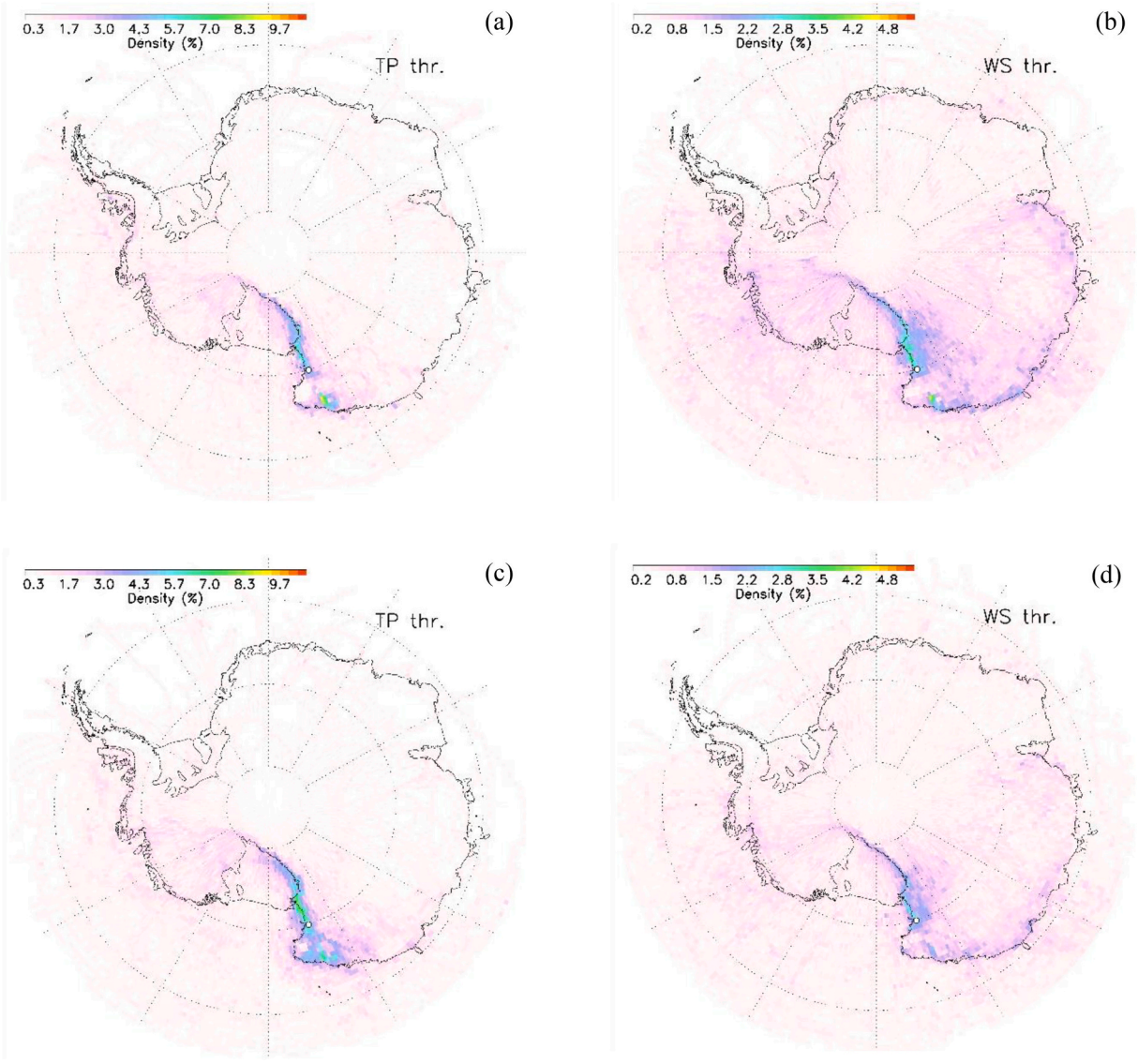

Fig. 5. Panel (a) and (c): percentage of the air mass back-trajectories (TJs) associated with precipitation values higher than the threshold of 50th percentile of the precipitation data distribution for Larsen Glacier (0.0095 mm w.e.) and Tourmaline Plateau (0.008 mm w.e.), respectively. Panel (b) and (d): percentage of the TJs associated with wind speed values higher than the threshold of 50th percentile of the wind data distribution for Larsen Glacier (10.4 ms^{-1}) and Tourmaline Plateau (2.1 ms^{-1}), respectively. TJs were calculated for the whole sampling period.

Table 3
Correlation matrix (Spearman's coefficients) among meteorological parameters, depositional fluxes, and MPs characteristics ($n = 6$). Significant correlations ($p \leq 0.05$) are marked with asterisks.

	Flux									
Flux	1.00	Size								
Size	0.32	1.00	Dark							
Dark	−0.26	−0.99*	1.00	Light						
Light	0.26	0.99*	−1.00	1.00	T					
T	−0.83*	−0.38	0.26	−0.26	1.00	P				
P	−0.89*	−0.64	0.60	−0.60	0.71	1.00	RU			
RU	−0.43	−0.46	0.54	−0.54	0.26	0.60	1.00	Wind Speed		
Wind Speed	0.71	−0.32	0.37	−0.37	0.60	−0.31	−0.09	1.00	NSW	
NSW	−0.54	−0.14	−0.09	−0.09	0.37	0.66	0.09	−0.09	1.00	EWW
EWW	−0.83*	−0.06	0.03	−0.03	0.60	0.54	0.26	−0.89*	0.09	1.00

(2019), and a settling velocity of 0.029 ms^{-1} (as calculated in the work of Illuminati et al., 2020 for particles of 2.5–10 μm), we estimated a dispersion of ~600 km from the source for mean daily wind speeds of 16 ms^{-1}, recorded at Larsen Glacier and Tourmaline Plateau. It should not be excluded that distances greater than 600 km could be reached, particularly if we consider that during winter, katabatic winds can blow with gusts up to 80 m s^{-1}. Similar distances were observed in other regions (Welsh et al., 2022); however, caution is warranted in

interpreting these results on MP, as suggested by Wright et al. (2020), due to various assumptions (size/aerodynamic equivalent diameter, density, settling velocity) made about particle behaviour and meteorological conditions. Therefore, further research is required to enhance this evidence base.

Considering the TJ's main pathways of the MP's mean residence time in the atmosphere and the meteorological parameters, we hypothesize that MPs collected at Larsen Glacier may result from a combination of various atmospheric transport mechanisms. Direct, fast transport processes associated with wet deposition could resuspend plastic material from the nearby coastal area of MZS or from the McMurdo Sound (~300–400 km away), along the Transantarctic Mountains. Conversely, slow, long-range transport associated with katabatic wind events, might carry particles from the Antarctic plateau. The morphological characteristics and position of the Tourmaline Plateau, along with less intense katabatic winds may explain a more significant contribution from short-range transport processes, resuspending plastic material from nearby research stations, like the Italian MZS and the south-Korean Jan Bogo Station. Nevertheless, due to the low temporal resolution (nine to ten months of sampling), TJs served more as an instrument to understand potential air mass transport than for exact MP tracking.

4. Conclusions

This study provides the first evidence of microplastic pollution in atmospheric deposition collected directly along the coastal region of Victoria Land. Using passive bulk samplers and RMS, MPs were detected in six of the seven samples, primarily as polypropylene fragments, averaging a deposition rate of 1.7 ± 1.1 MPs m^{-2} d^{-1}. Microplastics found in coastal sites are likely influenced by local sources, potentially linked to human activities at nearby research stations. The HYSPLIT model and a negative correlation with wind direction suggest Antarctic plateau as a possible MP source for remote sites like Larsen Glacier and Tourmaline Plateau.

These findings contribute to the growing body of evidence that microplastics are pervasive pollutants, even in remote and pristine environments like Antarctica. Further research with improved temporal resolution and standardized protocols is essential to fully understand the pathways and impacts of microplastics in the Antarctic environment.

CRediT authorship contribution statement

Silvia Illuminati: Writing – original draft, Visualization, Project administration, Methodology, Conceptualization. **Valentina Notarstefano:** Writing – review & editing, Validation, Methodology. **Chiara Tinari:** Investigation, Conceptualization. **Matteo Fanelli:** Data curation. **Federico Girolametti:** Validation. **Behixhe Ajdini:** Visualization. **C. Scarchilli:** Resources, Investigation. **V. Ciardini:** Methodology. **A. Iaccarino:** Software, Data curation. **E. Giorgini:** Supervision, Resources. **A. Annibaldi:** Writing – review & editing, Supervision, Funding acquisition. **C. Truzzi:** Writing – review & editing, Supervision.

Declaration of competing interest

The authors declare the following financial interests/personal relationships which may be considered as potential competing interests: Valentina Notarstefano reports financial support was provided by European Union. Silvia Illuminati reports travel and writing assistance were provided by European Union. Anna Annibaldi reports travel and writing assistance were provided by European Union. Silvia Illuminati reports a relationship with Italian Ministry of Universities and Research that includes: travel reimbursement. If there are other authors, they declare that they have no known competing financial interests or personal relationships that could have appeared to influence the work reported in this paper.

Data availability

MPs data will be made available on request by asking to the corresponding author at the e-mail address: s.illuminati@staff.univpm.it.

Meteorological dataset and information are achieved by the Italian Antarctic Meteo-Climatological Observatory (IAMCO) of the PNRA and are freely downloadable from https://www.climantartide.it. ECMWF ERA5 reanalysis data are freely available on Copernicus Climate Change Service (C3S) Climate Data Store (CDS) under: doi:10.24381/cds.bd0915c6 and doi:10.24381/cds.adbb2d47.

Acknowledgments

The authors gratefully acknowledge the Antarctic Technical Unit of the National Agency for New Technologies, Energy and Sustainable Economic Development (ENEA) for logistic support. The authors Silvia Illuminati, Valentina Notarstefano and Anna Annibaldi acknowledge financial support from the European Union—Next Generation EU (project code: ECS00000041; project title: Innovation, digitalization and sustainability for the diffused economy in Central Italy—VITALITY). The corresponding author Silvia Illuminati acknowledge financial support for travel reimbursement from the National Progamme of Antarctic Research (PNRA), within the framework of the Project PNRA 2015/AZ3.01: "Spatial and temporal (intra- and inter-annual) evolution of the chemical composition of the aerosol in the Victoria Land (Antarctica) in relation with local and long-range transport processes".

Appendix A. Supplementary data

The following materials are available in the Supplementary Materials: **Text S1**: Evolution of the principal meteorological parameters during the sampling period. **Fig. S1-S6**: Seasonal evolution of the main meteorological parameters recorded in the different sampling sites; **Fig. S7**: The year-round evolution of snow accumulation at Larsen Glacier reported together with the main meteorological parameters. **Fig. S8**: Air-mass back-trajectories arriving at (a) Larsen Glacier and (b) Tourmaline Plateau calculated for the whole sampling period; **Table S1**: Microphotographs and Raman spectra of the identified MPs. Supplementary data to this article can be found online at https://doi.org/10.1016/j.scitotenv.2024.175221.

References

Abbasi, S., Turner, A., 2021. Dry and wet deposition of microplastics in a semi-arid region (Shiraz, Iran). Sci. Total Environ. 786, 147358 https://doi.org/10.1016/j.scitotenv. 2021.147358.

Abbasi, S., Keshavarzi, B., Moore, F., Turner, A., Kelly, F.J., Dominguez, A.O., Jaafarzadeh, N., 2019. Distribution and potential health impacts of microplastics and microrubbers in air and street dusts from Asaluyeh County. Iran. Environ. Pollut. 244, 153–164. https://doi.org/10.1016/j.envpol.2018.10.039.

Absher, T.M., Ferreira, S.L., Kern, Y., Ferreira, A.L., Christo, S.W., Ando, R.A., 2019. Incidence and identification of microfibres in ocean waters in Admiralty Bay. Antarctica. Environ. Sci. Pollut. Res. 26, 292–298. https://doi.org/10.1007/s11356-018-3509-6.

Allen, S., Allen, D., Moss, K., Le Roux, G., Phoenix, V.R., Sonke, J.E., 2020. Examination of the ocean as a source for atmospheric microplastics. PLoS One 15, 1–14. https://doi.org/10.1371/journal.pone.0232746.

Allen, S., Allen, D., Phoenix, V.R., Le Roux, G., Durántez Jiménez, P., Simonneau, A., Binet, S., Galop, D., 2019. Atmospheric transport and deposition of microplastics in a remote mountain catchment. Nat. Geosci. 12, 339–344. https://doi.org/10.1038/s41561-019-0335-5.

Ambrosini, R., Azzoni, R.S., Pittino, F., Diolaiuti, G., Franzetti, A., Parolini, M., 2019. First evidence of microplastic contamination in the supraglacial debris of an alpine glacier. Environ. Pollut. 253, 297–301. https://doi.org/10.1016/j.envpol.2019.07.005.

Amodio, M., Catino, S., Dambruoso, P.R., de Gennaro, G., Di Giglio, A., Giungato, P., Laiola, E., Marzocca, A., Mazzone, A., Sardaro, A., Tutino, M., 2014. Atmospheric Deposition : Sampling Procedures , Analytical Methods, and Main Recent Findings from the Scientific Literature. Adv. Meteorol. 5, 1590–1602.

Aves, A.R., Revell, L.E., Gaw, S., Ruffell, H., Schuddeboom, A., Wotherspoon, N.E., Larue, M., Mcdonald, A.J., 2022. First evidence of microplastics in Antarctic snow. Cryosphere 16, 2127–2145. https://doi.org/10.5194/tc-16-2127-2022.

Bank, M.S., Hansson, S.V., 2019. The plastic cycle: a novel and holistic paradigm for the Anthropocene. Environ. Sci. Technol. 53, 7177–7179. https://doi.org/10.1021/acs.est.9b02942.

Becagli, S., Marchese, C., Caiazzo, L., Ciardini, V., Lazzara, L., Mori, G., Nuccio, C., Scarchilli, C., Severi, M., Traversi, R., 2022. Biogenic aerosol in central East Antarctic plateau as a proxy for the ocean-atmosphere interaction in the Southern Ocean. Sci. Total Environ. 810, 151285 https://doi.org/10.1016/j.scitotenv.2021.151285.

Bergami, E., Manno, C., Cappello, S., Vannuccini, M.L., Corsi, I., 2020a. Nanoplastics affect moulting and faecal pellet sinking in Antarctic krill (*Euphausia superba*) juveniles. Environ. Int. 143, 105999 https://doi.org/10.1016/j.envint.2020.105999.

Bergami, E.a, Rota, E., Caruso, T., Birarda, G., Vaccari, L., Corsi, I., 2020b. Plastics everywhere: first evidence of polystyrene fragments inside the common Antarctic collembolan *Cryptopygus antarcticus*. Biol. Lett. 16 https://doi.org/10.1098/rsbl.2020.0093.

Bergmann, M., Mützel, S., Primpke, S., Tekman, M.B., Trachsel, J., Gerdts, G., 2019. White and wonderful? Microplastics prevail in snow from the Alps to the Arctic. Sci. Adv. 5, 1–11. https://doi.org/10.1126/sciadv.aax1157.

Bertinetti, S., Berto, S., Malandrino, M., Vione, D., Abollino, O., Conca, E., Marafante, M., Annibaldi, A., Truzzi, C., Illuminati, S., 2022. Chemical speciation of Antarctic atmospheric depositions. Appl. Sci. 12, 1–21. https://doi.org/10.3390/app12094438.

Bessa, F., Ratcliffe, N., Otero, V., Sobral, P., Marques, J.C., Waluda, C.M., Trathan, P.N., Xavier, J.C., 2019. Microplastics in gentoo penguins from the Antarctic region. Sci. Rep. 9, 1–7. https://doi.org/10.1038/s41598-019-50621-2.

Bianco, A., Sordello, F., Ehn, M., Vione, D., Passananti, M., 2020. Degradation of nanoplastics in the environment: reactivity and impact on atmospheric and surface waters. Sci. Total Environ. 742, 140413 https://doi.org/10.1016/j.scitotenv.2020.140413.

Brahney, J., Hallerud, M., Heim, E., Hahnenberger, M., Sukumaran, S., 2020. Plastic rain in protected areas of the United States. Science 80-.). 368, 1257–1260. https://doi.org/10.1126/science.aaz5819.

Brahney, J., Mahowald, N., Prank, M., Cornwell, G., Klimont, Z., Matsui, H., Prather, K. A., 2021. Constraining the atmospheric limb of the plastic cycle. Proc. Natl. Acad. Sci. USA 118, 1–10. https://doi.org/10.1073/pnas.2020719118.

Cai, L., Wang, J., Peng, J., Tan, Z., Zhan, Z., Tan, X., Chen, Q., 2017. Characteristic of microplastics in the atmospheric fallout from Dongguan city, China: preliminary research and first evidence. Environ. Sci. Pollut. Res. 24, 24928–24935. https://doi.org/10.1007/s11356-017-0116-x.

Chen, L., Peng, S., Liu, J., Hou, Q., 2012. Dry deposition velocity of total suspended particles and meteorological influence in four locations in Guangzhou. China. J. Environ. Sci. 24, 632–639. https://doi.org/10.1016/S1001-0742(11)60805-X.

Cincinelli, A., Scopetani, C., Chelazzi, D., Lombardini, E., Martellini, T., Katsoyiannis, A., Fossi, M.C., Corsolini, S., 2017. Microplastic in the surface waters of the Ross Sea (Antarctica): occurrence, distribution and characterization by FTIR. Chemosphere 175, 391–400. https://doi.org/10.1016/j.chemosphere.2017.02.024.

Cole, M., Lindeque, P., Halsband, C., Galloway, T.S., 2011. Microplastics as contaminants in the marine environment: a review. Mar. Pollut. Bull. 62, 2588–2597. https://doi.org/10.1016/j.marpolbul.2011.09.025.

Cunningham, E.M., Ehlers, S.M., Dick, J.T.A., Sigwart, J.D., Linse, K., Dick, J.J., Kiriakoulakis, K., 2020. High abundances of microplastic pollution in Deep-Sea sediments: evidence from Antarctica and the Southern Ocean. Environ. Sci. Technol. 54, 13661–13671. https://doi.org/10.1021/acs.est.0c03441.

Dong, M., Zhang, Q., Xing, X., Chen, W., She, Z., Luo, Z., 2020. Raman spectra and surface changes of microplastics weathered under natural environments. Sci. Total Environ. 739, 139990 https://doi.org/10.1016/j.scitotenv.2020.139990.

Dris, R., Gasperi, J., Saad, M., Mirande, C., Tassin, B., 2016. Synthetic fibres in atmospheric fallout: a source of microplastics in the environment? Mar. Pollut. Bull. 104, 290–293. https://doi.org/10.1016/j.marpolbul.2016.01.006.

Evangeliou, N., Grythe, H., Klimont, Z., Heyes, C., Eckhardt, S., Lopez-Aparicio, S., Stohl, A., 2020. Atmospheric transport is a major pathway of microplastics to remote regions. Nat. Commun. 11 https://doi.org/10.1038/s41467-020-17201-9.

Faraji, M., Pourpak, Z., Naddafi, K., Nodehi, R.N., Nicknam, M.H., Shamsipour, M., Rezaei, S., Ghozikali, M.G., Ghanbarian, M., Mesdaghinia, A., 2018. Effects of airborne particulate matter (PM10) from dust storm and thermal inversion on global DNA methylation in human peripheral blood mononuclear cells (PBMCs) in vitro. Atmos. Environ. 195, 170–178. https://doi.org/10.1016/j.atmosenv.2018.09.042.

Geyer, R., Jambeck, J.R., Law, K.L., 2017. Production, use, and fate of all plastics ever made. Sci. Adv. 3, 25–29. https://doi.org/10.1126/sciadv.1700782.

González-Pleiter, M., Edo, C., Velázquez, D., Casero-Chamorro, M.C., Leganés, F., Quesada, A., Fernández-Piñas, F., Rosal, R., 2020. First detection of microplastics in the freshwater of an Antarctic specially protected area. Mar. Pollut. Bull. 161, 1–6. https://doi.org/10.1016/j.marpolbul.2020.111811.

González-Pleiter, M., Lacerot, G., Edo, C., Pablo Lozoya, J., Legane, acute, F.S., Fernández-Pinãs, F., Rosal, R., Teixeira-De-Mello, F., 2021. A pilot study about microplastics and mesoplastics in an Antarctic glacier. Cryosphere 15, 2531–2539. https://doi.org/10.5194/tc-15-2531-2021.

Hersbach, H., Bell, B., Berrisford, P., Hirahara, S., Horányi, A., Muñoz-Sabater, J., Nicolas, J., Peubey, C., Radu, R., Schepers, D., Simmons, A., Soci, C., Abdalla, S., Abellan, X., Balsamo, G., Bechtold, P., Biavati, G., Bidlot, J., Bonavita, M., De Chiara, G., Dahlgren, P., Dee, D., Diamantakis, M., Dragani, R., Flemming, J., Forbes, R., Fuentes, M., Geer, A., Haimberger, L., Healy, S., Hogan, R.J., Hólm, E., Janisková, M., Keeley, S., Laloyaux, P., Lopez, P., Lupu, C., Radnoti, G., de Rosnay, P., Rozum, I., Vamborg, F., Villaume, S., Thépaut, J.N., 2020. The ERA5 global reanalysis. Q. J. R. Meteorol. Soc. 146, 1999–2049. https://doi.org/10.1002/qj.3803.

Ibañez, A.E., Morales, L.M., Torres, D.S., Borghello, P., Haidr, N.S., Montalti, D., 2020. Plastic ingestion risk is related to the anthropogenic activity and breeding stage in an Antarctic top predator seabird species. Mar. Pollut. Bull. 157, 111351 https://doi.org/10.1016/j.marpolbul.2020.111351.

Illuminati, S., Annibaldi, A., Bau, S., Scarchilli, C., Ciardini, V., Grigioni, P., Girolametti, F., Vagnoni, F., Scarponi, G., Truzzi, C., 2020. Seasonal evolution of size-segregated particulate mercury in the atmospheric aerosol over Terra Nova Bay. Antarctica. Molecules 25. https://doi.org/10.3390/molecules25173971.

Illuminati, S., Bau, S., Annibaldi, A., Mantini, C., Libani, G., Truzzi, C., Scarponi, G., 2016. Evolution of size-segregated aerosol mass concentration during the Antarctic summer at northern foothills. Victoria Land. Atmos. Environ. 125 https://doi.org/10.1016/j.atmosenv.2015.11.015.

Isobe, A., Uchiyama-Matsumoto, K., Uchida, K., Tokai, T., 2017. Microplastics in the Southern Ocean. Mar. Pollut. Bull. 114, 623–626. https://doi.org/10.1016/j.marpolbul.2016.09.037.

Klein, M., Fischer, E.K., 2019. Microplastic abundance in atmospheric deposition within the metropolitan area of Hamburg. Germany. Sci. Total Environ. 685, 96–103. https://doi.org/10.1016/j.scitotenv.2019.05.405.

Lacerda, A.L. d.F., Rodrigues, L. dos S. van Sebille, E., Rodrigues, F.L., Ribeiro, L., Secchi, E.R., Kessler, F., Proietti, M.C., 2019. Plastics in sea surface waters around the Antarctic peninsula. Sci. Rep. 9, 1–12. doi:https://doi.org/10.1038/s41598-019-40311-4.

Lee, G., Ahn, J., Ju, H., Ritterbusch, F., Oyabu, I., Buizert, C., Kim, S., Moon, J., Ghosh, S., Kawamura, K., Lu, Z.-T., Hong, S., Han, C.H., Hur, S.D., Jiang, W., Yang, G.-M., 2021. Chronostratigraphy of the Larsen blue-ice area in northern Victoria Land, East Antarctica, and its implications for paleoclimate. Cryosphere 16, 2301–2324. https://doi.org/10.5194/tc-16-2301-2022, 2022.

Liu, K., Wang, X., Fang, T., Xu, P., Zhu, L., Li, D., 2019a. Source and potential risk assessment of suspended atmospheric microplastics in Shanghai. Sci. Total Environ. 675, 462–471. https://doi.org/10.1016/j.scitotenv.2019.04.110.

Liu, K., Wu, T., Wang, X., Song, Z., Zong, C., Wei, N., Li, D., 2019b. Consistent transport of terrestrial microplastics to the ocean through atmosphere. Environ. Sci. Technol. 53, 10612–10619. https://doi.org/10.1021/acs.est.9b03427.

Montano, L., Giorgini, E., Notarstefano, V., Notari, T., Ricciardi, M., Piscopo, M., Motta, O., 2023. Raman Microspectroscopy evidence of microplastics in human semen. Sci. Total Environ. 901, 165922 https://doi.org/10.1016/j.scitotenv.2023.165922.

Munari, C., Infantini, V., Scoponi, M., Rastelli, E., Corinaldesi, C., Mistri, M., 2017. Microplastics in the sediments of Terra Nova Bay (Ross Sea, Antarctica). Mar. Pollut. Bull. 122, 161–165. https://doi.org/10.1016/j.marpolbul.2017.06.039.

Pironti, C., Notarstefano, V., Ricciardi, M., Motta, O., Giorgini, E., Montano, L., 2023. First evidence of microplastics in human urine, a preliminary study of intake in the human body. Toxics 11, 1–9. https://doi.org/10.3390/toxics11010040.

PlasticsEurope, 2019. Plastics—The Facts 2019: An Analysis of European Plastics Production, Demand and Waste Data. PlasticsEurope.

Ragusa, A., Notarstefano, V., Svelato, A., Belloni, A., Gioacchini, G., Blondeel, C., Zucchelli, E., De Luca, C., D'avino, S., Gulotta, A., Carnevali, O., Giorgini, E., 2022. Raman Microspectroscopy detection and characterisation of microplastics in human breastmilk. polymers (Basel). 14, 1–14. https://doi.org/10.3390/polym14132700.

Ragusa, A., Svelato, A., Santacroce, C., Catalano, P., Notarstefano, V., Carnevali, O., Papa, F., Rongioletti, M.C.A., Baiocco, F., Draghi, S., D'Amore, E., Rinaldo, D., Matta, M., Giorgini, E., 2021. Plasticenta: first evidence of microplastics in human placenta. Environ. Int. 146, 106274 https://doi.org/10.1016/j.envint.2020.106274.

Roblin, B., Ryan, M., Vreugdenhil, A., Aherne, J., 2020. Ambient atmospheric deposition of anthropogenic microfibres and microplastics on the Western periphery of Europe (Ireland). Environ. Sci. Technol. 54, 11100–11108. https://doi.org/10.1021/acs.est.0c04000.

Rolph, G., Stein, A., Stunder, B., 2017. Real-time environmental applications and display sYstem: READY. Environ. Model Softw. 95, 210–228 (accessed on 1 July 2023). https://doi.org/10.1016/j.envsoft.2017.06.025.

Scarchilli, C., Ciardini, V., Grigioni, P., Iaccarino, A., De Silvestri, L., Proposito, M., Dolci, S., Camporeale, G., Schioppo, R., Antonelli, A., Baldini, L., Roberto, N., Argentini, S., Bracci, A., Frezzotti, M., 2020. Characterization of snowfall estimated by in situ and ground-based remote-sensing observations at Terra Nova Bay, Victoria land. Antarctica. J. Glaciol. 66, 1006–1023. https://doi.org/10.1017/jog.2020.70.

Scarchilli, C., Frezzotti, M., Grigioni, P., De Silvestri, L., Agnoletto, L., Dolci, S., 2010. Extraordinary blowing snow transport events in East Antarctica. Clim. Din. 34, 1195–1206. https://doi.org/10.1007/s00382-009-0601-0.

Scarchilli, C., Frezzotti, M., Ruti, P.M., 2011. Snow precipitation at four ice core sites in East Antarctica: provenance, seasonality and blocking factors. Clim. Dyn. 37, 2107–2125. https://doi.org/10.1007/s00382-010-0946-4.

Schlosser, E., Oerter, H., Masson-Delmotte, V., Reijmer, C., 2008. Atmospheric influence on the deuterium excess signal in polar firn: implication for ice-core interpretation. J. Glaciol. 54, 117–124. https://doi.org/10.3189/002214308784408991.

Schwabl, P., Koppel, S., Konigshofer, P., Bucsics, T., Trauner, M., Reiberger, T., Liebmann, B., 2019. Detection of various microplastics in human stool: a prospective case series. Ann. Intern. Med. 171, 453–457. https://doi.org/10.7326/M19-0618.

Sfriso, A.A., Tomio, Y., Rosso, B., Gambaro, A., Sfriso, A., Corami, F., Rastelli, E., Corinaldesi, C., Mistri, M., Munari, C., 2020. Microplastic accumulation in benthic invertebrates in Terra Nova Bay (Ross Sea, Antarctica). Environ. Int. 137, 105587 https://doi.org/10.1016/j.envint.2020.105587.

SLOPP Library of microplastics. Available online: https://rochmanlab.com/slopp-and-slopp-e-raman-spectral-libraries-formicroplastics-research (accessed on 1 February 2023).

Stein, A.F., Draxler, R.R., Rolph, G.D., Stunder, B.J.B., Cohen, M.D., Ngan, F., 2015. NOAA's HYSPLIT atmospheric transport and dispersion modeling system. Bull. Am. Meteorol. Soc. 96, 2059–2077. https://doi.org/10.1175/BAMS-D-14-00110.1.

Suaria, G., Perold, V., Lee, J.R., Lebouard, F., Aliani, S., Ryan, P.G., 2020. Floating macro- and microplastics around the Southern Ocean: results from the Antarctic circumnavigation expedition. Environ. Int. 136, 105494 https://doi.org/10.1016/j.envint.2020.105494.

Szewc, K., Graca, B., Dołęga, A., 2021. Atmospheric deposition of microplastics in the coastal zone: characteristics and relationship with meteorological factors. Sci. Total Environ. 761 https://doi.org/10.1016/j.scitotenv.2020.143272.

Tatsii, D., Bucci, S., Taraprasad, B., Guettler, J., Bakels, L., Bagheri, G., Stohl, A., 2024. Shape matters: long-range transport of microplastic fibers in the atmosphere. Environ. Sci. Technol. 58, 671. https://doi.org/10.1021/acs.est.3c08209.

Truong, T.N.S., Strady, E., Kieu-Le, T.C., Tran, Q.V., Le, T.M.T., Thuong, Q.T., 2021. Microplastic in atmospheric fallouts of a developing southeast Asian megacity under tropical climate. Chemosphere 272, 129874. https://doi.org/10.1016/j.chemosphere.2021.129874.

Vagnoni, F., Illuminati, S., Annibaldi, A., Memmola, F., Giglione, G., Falgiani, A.M., Girolametti, F., Fanelli, M., Scarponi, G., Truzzi, C., 2021. Seasonal evolution of the chemical composition of atmospheric aerosol in Terra Nova Bay (Antarctica). Atmosphere 12, 1030. https://doi.org/10.3390/atmos12081030.

Vicente, J.S., Gejo, J.L., Rothenbacher, S., Sarojiniamma, S., Gogritchiani, E., Wörner, M., Kasper, G., Braun, A.M., 2009. Oxidation of polystyrene aerosols by VUV-photolysis and/or ozone. Photochem. Photobiol. Sci. 8, 944–952. https://doi.org/10.1039/b902749a.

Waller, C.L., Griffiths, H.J., Waluda, C.M., Thorpe, S.E., Loaiza, I., Moreno, B., Pacherres, C.O., Hughes, K.A., 2017. Microplastics in the Antarctic marine system: an emerging area of research. Sci. Total Environ. 598, 220–227. https://doi.org/10.1016/j.scitotenv.2017.03.283.

Wang, X., Li, C., Liu, K., Zhu, L., Song, Z., Li, D., 2020. Atmospheric microplastic over the South China Sea and East Indian Ocean: abundance, distribution and source. J. Hazard. Mater. 389, 121846 https://doi.org/10.1016/j.jhazmat.2019.121846.

Welsh, B., Aherne, J., Paterson, A.M., Yao, H., McConnell, C., 2022. Atmospheric deposition of anthropogenic particles and microplastics in south-Central Ontario. Canada. Sci. Total Environ. 835, 155426 https://doi.org/10.1016/j.scitotenv.2022.155426.

Wright, S.L., Ulke, J., Font, A., Chan, K.L.A., Kelly, F.J., 2020. Atmospheric microplastic deposition in an urban environment and an evaluation of transport. Environ. Int. 136, 105411 https://doi.org/10.1016/j.envint.2019.105411.

Wu, WM., Yang, J. & Criddle, C.S. 2017. Microplastics pollution and reduction strategies. Front. Environ. Sci. Eng. 11, 6. doi:https://doi.org/10.1007/s11783-017-0897-7.

Zhang, Y., Gao, T., Kang, S., Allen, S., Luo, X., Allen, D., 2021. Microplastics in glaciers of the Tibetan plateau: evidence for the long-range transport of microplastics. Sci. Total Environ. 758, 143634 https://doi.org/10.1016/j.scitotenv.2020.143634.